

Composite Fermion states on the torus

M. Hermanns¹

¹*Institute for Theoretical Physics of Cologne, 50937 Cologne, Germany*

(Dated: April 17, 2013)

We extend the composite fermion construction to the torus geometry. We verify the validity of our construction by computing the overlap of the composite fermion state to the exact diagonalization ground state of both Coulomb interaction and Haldane-pseudopotential interaction V_0 (V_1) for bosonic (fermionic) states.

PACS numbers: 73.43.-f

I. INTRODUCTION

A paramount impetus for the growing interest in strongly correlated quantum matter is the discovery that such systems can be topologically ordered. The first, and most prominent, examples are the various incompressible fractional quantum Hall (FQH) liquids. These are formed at low temperatures, when very clean two-dimensional electron gases are subjected to a strong perpendicular magnetic field [1]. The most striking consequence of the topological order in the FQH liquids is that the emergent low-energy quasiparticles have fractional electric charge, and are believed to obey fractional braiding statistics [2]. Another hallmark of a topological phase of matter is that the number of degenerate ground states depend on the topology of the space on which the state is defined. Again, the simplest example are the FQH liquids, where numerical solutions of the microscopic Coulomb problem can be compared to different theoretical predictions. In this paper we develop techniques that makes it possible to make such comparisons for the Jain states, which are an important set of actually observed FQH liquids.

The problem of many particles moving in a strong magnetic field, and interacting via Coulomb forces, is intractable, so one has to find an effective description. While a natural approach is to construct effective low-energy field theories [3], a very fruitful alternative route — following a seminal article by Laughlin [4] — has been to construct model wave functions with well defined topological properties, and verify numerically that they describe small systems accurately. The most common method of verification is to compute the overlap with the exact Coulomb ground state, but recently it was shown that studying the entanglement spectrum [5] can give valuable complementary insights.

Although most effort in FQH physics during the last decade has been aimed at understanding different non-abelian states, we shall here concentrate on the family of observed states in the lowest Landau level. There are two successful theoretical approaches to describe these states — the Haldane-Halperin hierarchy [6, 7] and the composite fermion (CF) theory [8].

The Haldane-Halperin hierarchy describes a family of incompressible FQH liquids formed via successive condensation of the low-energy excitations — quasiholes and

quasielectrons. It predicts that incompressible FQH liquids may be found at filling fractions $\nu = p/q$, where p and q are relatively prime integers and q is odd. It also argues that the stability of the liquids decreases roughly as $\sim 1/q$ with increasing denominator. The emergent quasiparticles have fractional electric charge $1/q$ and obey fractional abelian braiding statistics. The simplest way to obtain explicit wave functions for ground and quasiparticle states, at all levels of the hierarchy, is by using conformal field theory techniques [9, 10].

The CF theory can describe most of the observed FQH liquids by mapping the problem of strongly interacting fermions that fill a fraction ν of a Landau level, to that of non-interacting (or at least weakly-interacting) composite fermions filling an integer number of effective Landau levels in a reduced magnetic field. The latter describes an incompressible state because of the finite gap between the effective Landau levels. This approach also gives a simple picture of the ground state and the low-energy sector. A big initial success of the CF theory was the very good agreement with the exact Coulomb eigenstates obtained from finite-size numerical studies, both for the ground state and the excited states. It was later shown that for the important case of the positive Jain series, the hierarchy wave functions exactly coincide with those from CF theory, both in planar and spherical geometry [11–13]. The two approaches also give very similar predictions for the relative stability of the various FQH liquids.

Both approaches to the abelian FQH states in the lowest Landau level — the hierarchy and the CF theory — are well-understood (and studied) in the disk and sphere geometry, see eg. [14] and references therein. The torus geometry, however, has been studied far less and explicit wave function were only known for certain model states, that are determined uniquely (up to center-of-mass translations) by their vanishing properties [15–17]. A first attempt to construct hierarchical wave functions on the torus was done in Ref. [18] using conformal field theory techniques. While it provided wave functions that are very good approximations to the exact Coulomb ground state in a certain parameter regime, the construction was not satisfactory in that the wave functions did not transform properly under modular transformations and were uniquely defined only in the thermodynamic limit. It has only recently been understood how to resolve these problems [19].

In this paper, we show how to generalize the CF construction to the torus geometry. The construction has no free parameters and gives unique model wave functions (up to center-of-mass translations) of the ground state and the excited states at filling fraction $\nu = \frac{n}{np+1}$, n and p integers, corresponding to the positive Jain series.

There are several reasons, why the torus geometry is interesting, even though it cannot be realized experimentally. We already mentioned the topological ground state degeneracy, but it is also important that numerical calculations are better defined on closed manifolds, such as the sphere and the torus, since they do not suffer from edge effects, which can be substantial for the system sizes one can reach numerically. While numerics on the sphere have proven very useful, there are still problems connected to finite size, most notably the so-called shift. It can happen that two states that are at the same (thermodynamic) filling fraction ν appear at different magnetic fluxes N_ϕ in the finite-size system. The most prominent examples are the Moore-Read state [20] and the CF Fermi liquid [21], which are both at filling 1/2 but have different shift. Numerical comparison of these two states on the sphere is therefore only indirect. On the torus, this issue does not arise, which allows for a direct comparison of these states [22].

Another advantage of the torus geometry is that one can change the shape of the torus—described by the modular parameter τ —and thus get more information about a state without having to increase the system size. This was successfully used for entanglement entropy calculations, where one wants to extract a subleading constant term in the entropy. Ref. [23] showed that changing the aspect ratio of the torus and thus obtaining additional data, yielded much more accurate bounds on the topological constant than could be obtained from sphere calculations. Also, as shown by Avron et.al. [24], by studying the response of QH liquid to an adiabatic change in τ , one can determine the odd part of the viscosity tensor. An explicit calculation in the case of the Laughlin states was made by Read [25], and the results in this paper could be used to perform similar calculations for the Jain states. Let us also note that the techniques introduced in this manuscript are not restricted to the positive Jain series, but can also be used to study more exotic states, such as the BS states [26], the NAC states [27], as well as the closely related bipartite CF states [28].

Outline of the manuscript In Section II we first present the CF construction on the disk geometry and show how to generalize the approach to the torus geometry. We discuss single-particle states on the torus in Subsection II B and give an expression for the product of two such states at different magnetic fluxes N_{ϕ_1} and N_{ϕ_2} in Subsection II C. The derivation of this identity is given in Appendix A. In Subsection II D we show how to evaluate CF states on the torus. Overlaps of some CF states with exact diagonalization results using both Coulomb and Haldane pseudo-potential interactions are calculated in Section III. These overlaps should be regarded solely

as a proof of principle that the construction on the torus is sound. In Section IV, we speculate on possible lowest Landau level projection schemes in real space, given that the torus places additional constraints on model wave functions.

II. GENERAL COMPOSITE FERMION CONSTRUCTION

In this Section we explain how to generalize the CF construction to the torus geometry. In Subsection II A we first discuss the CF construction on the disk and sphere and point out some subtleties that become important on the torus. Subsection II B contains a short review on the single-particle states on the torus. In Subsection II C, we derive formulas for the projection of a product of two single-particle states. In Subsection II D, we discuss properties of the CF states on the torus using the bosonic CF state at $\nu = 2/3$ as an explicit example.

A. Composite fermions on the disk geometry

There are already many good texts on the CF construction—see for instance [14] for an extensive and pedagogical review. Thus, we keep the discussion in this section very brief and focus on properties that are relevant for the torus. In the following, we restrict ourselves to the positive Jain series at fillings $\nu = \frac{n}{np+1}$, where $n \geq 1$ and p are integers. We expect the negative Jain series to work analogously, but we have not yet performed any explicit calculations. In the CF theory, one attaches an even (odd) number of vortices to strongly interacting fermions (bosons). The resulting fermionic particles are called composite fermions and one assumes that these composite particles are non-interacting or at least very weakly interacting. Due to the attachment of vortices, they feel a reduced magnetic field $B^* = B - p\rho\phi_0$, where ϕ_0 is the magnetic flux quantum and ρ is the two-dimensional density. For properly chosen p the reduction of magnetic flux is such that the CFs fill an integer number of effective Landau levels.

A trial wave function for the ground state of strongly interacting particles at filling $\nu = \frac{n}{np+1}$ is then usually written as

$$\Psi_\nu(\{z_j\}) = \mathcal{P}_{LLL} \left\{ \Phi_n(\{z_j\}) \cdot \prod_{i < j} (z_i - z_j)^p \right\}, \quad (1)$$

where $z = x + iy$ is a complex coordinate. $\Phi_n(\{z_j\})$ is the many-body wave function (slater determinant) for the n lowest Landau levels filled and \mathcal{P}_{LLL} projects to the lowest Landau level. Eq. (1) does not strictly speaking describe a proper lowest Landau level wave function on the disk, because it does not have the correct gaussian factor. Usually, one does not worry about this but just adds the correct factor by hand. However, this subtlety

becomes important on the torus as explained in the next paragraph.

The naive guess of how to generalize Eq. (1), is to replace each part by the respective torus counterpart. In particular, this would amount to replacing the Jastrow factor with its periodized version [15]

$$\prod_{i < j} (z_i - z_j)^p \rightarrow \prod_{i < j} \theta_1(z_i - z_j | \tau)^p, \quad (2)$$

where θ_1 is the odd Jacobi theta function (defined by setting $a = b = 1/2$ in Eq. (15)). We choose θ_1 because it is the only θ -function that has the correct short-distance behaviour, ie. is it the only antisymmetric θ -function. However, this choice poses two obvious problems: firstly, the wave function does not obey the correct boundary conditions on the torus, see Eq. (7). [37] Secondly, there is no efficient way to project the many-body wave function to the lowest Landau level. To the best of our knowledge, no analog of the Girvin-Jach projection [29] is known on the torus. We will comment more on this in section IV.

Instead of Eq. (1) we will consider the following expression:

$$\Psi_\nu(\{z_j\}) = \mathcal{P}_{LLL} \{ \Phi_n(\{z_j\}) \cdot \Phi_1(\{z_j\})^p \}. \quad (3)$$

The replacement of the Jastrow factor to Φ_1 is of course trivial for both the disk and sphere—in the former case it only differs by a gaussian factor. The point is, however, that (3) is a proper Landau level wave function on the disk, ie. it has the correct gaussian factor because the gaussian factors of Φ_n and Φ_1^p combine to give the correct factor at the combined flux. In addition, using expression (3) solves both the problems mentioned in the previous paragraph. It is straightforward to verify that $\Psi_\nu(\{z_j\})$ obeys the boundary conditions on the torus (7). The projection onto the lowest Landau level can be implemented on the single-particle level, which is explained in subsection II C.

B. Single-particle states on the torus

We consider a torus spanned by two, not necessarily orthogonal, translation vectors \vec{L}_1 and \vec{L}_2 . A homogeneous external magnetic field—perpendicular to the surface of the torus—is described in terms of the vector potential $\vec{A} = -By\hat{x}$ using Landau gauge. The number of flux quanta piercing the torus is related to the area $\mathcal{A} = |\vec{L}_1 \times \vec{L}_2|$ of the torus by $2\pi\ell_B^2 N_\phi = \mathcal{A} = L_1 L_2 \sin(\theta)$ with magnetic length $\ell_B = \sqrt{\hbar c/(eB)}$ and θ being the angle between \vec{L}_1 and \vec{L}_2 . The case of a rectangular torus corresponds to $\theta = \pi/2$. The shape of the torus is conveniently parametrized by the aspect ratio

$$\tau = \frac{L_2}{L_1} e^{i\theta}. \quad (4)$$

In the presence of the magnetic field, any valid wave function on the torus must be invariant (up to an overall

phase) under single-particle magnetic translations $t(\vec{L}_1)$ and $t(\vec{L}_2)$, where the magnetic translation operator is defined as

$$\hat{t}(\vec{L}) = \exp[\vec{L} \cdot (\vec{\nabla} - i\frac{e}{\hbar c} \vec{A}) - i\frac{\vec{L} \times \vec{r}}{\ell_B^2}]. \quad (5)$$

Let us define 'small' magnetic translations

$$\begin{aligned} \hat{t}_1 &\equiv \hat{t}\left(\frac{\vec{L}_1}{N_\phi}\right) = \exp\left[\frac{L_1}{N_\phi} \partial_x\right] \\ \hat{t}_2 &\equiv \hat{t}\left(\frac{\vec{L}_2}{N_\phi}\right) = \exp\left[i\pi \frac{L_2 \cos \theta}{L_1 N_\phi} + 2\pi i \frac{x}{L_1}\right] \\ &\quad \times \exp\left[\frac{L_2 \cos \theta}{N_\phi} \partial_x + \frac{L_2 \sin \theta}{N_\phi} \partial_y\right]. \end{aligned} \quad (6)$$

The periodic boundary conditions of a wave function ψ can, thus, be formulated as:

$$\begin{aligned} \hat{t}_1^{N_\phi} \psi &= e^{i\alpha_1} \psi \\ \hat{t}_2^{N_\phi} \psi &= e^{i\alpha_2} \psi. \end{aligned} \quad (7)$$

In the remainder of the manuscript, we will set the solenoid fluxes $\alpha_1, \alpha_2 = 0$ without loss of generality.

As \hat{t}_1 and \hat{t}_2 do not commute with each other, we can choose the single-particle states to be eigenstates of only one of them. In the following, we will mostly use eigenfunctions of \hat{t}_1

$$\begin{aligned} \phi_{n,j}^{\ell_B}(x, y) &= \mathcal{N}_n^{\ell_B} \sum_{k=-\infty}^{\infty} e^{-2\pi i(j+kN_\phi)z} e^{-y^2/(2\ell_B^2)} \\ &\times \exp\left[\frac{i\pi\tau}{N_\phi}(j+kN_\phi)^2\right] \cdot H_n\left(\frac{2\pi\ell_B}{L_1}(j+kN_\phi) - \frac{y}{\ell_B}\right), \end{aligned} \quad (8)$$

where $z = (x + iy)/L_1$ is the dimensionless complex coordinate of the particles, $n = 0, 1, \dots$ is the Landau level index and $j = 0, \dots, (N_\phi - 1)$ the momentum index. Note that the momentum is only defined modulo N_ϕ , because any larger value can be absorbed into the sum over windings around the torus. The normalization constant is given by

$$\mathcal{N}_n^{\ell_B} = \left(\frac{\sqrt{2N_\phi} \Im(\tau)}{(2^n n! \mathcal{A})} \right)^{1/2}, \quad (9)$$

where $\mathcal{A} = 2\pi\ell_B^2 N_\phi$ is the total area of the torus. $\phi_{n,j}^{\ell_B}$ is an eigenfunction of \hat{t}_1 with eigenvalue $\exp[-2\pi i j/N_\phi]$, while \hat{t}_2 shifts the momentum by one: $\hat{t}_2 \phi_{n,j}^{\ell_B} = \phi_{n,j-1}^{\ell_B}$. As we will need to distinguish single-particle states at different flux later on, we keep the magnetic length ℓ_B as an explicit parameter in the single-particle state $\phi_{n,j}^{\ell_B}$.

C. Product of single-particle states on the torus

In complete analogy to the disk and sphere geometry, we can write a product of two single-particle states on the torus at magnetic flux N_{ϕ_1} and N_{ϕ_2} as

$$\begin{aligned} & \phi_{n_1, j_1}^{\ell_1}(x, y) \cdot \phi_{n_2, j_2}^{\ell_2}(x, y) \\ &= \sum_{n=0}^{n_1+n_2} \sum_{j=0}^{N_{\phi}-1} C_{j_1, j_2; j}^{n_1, n_2; n} \cdot \phi_{n, j}^{\ell}(x, y), \quad (10) \end{aligned}$$

where the magnetic lengths are related by $\ell^{-2} = \ell_1^{-2} + \ell_2^{-2}$, which is equivalent to $N_{\phi} = N_{\phi_1} + N_{\phi_2}$. The constants $C_{j_1, j_2; j}^{n_1, n_2; n} = C_{j_1, j_2; j}^{n_1, n_2; n}(N_{\phi_1}, N_{\phi_2}, \tau)$ depend on the fluxes $N_{\phi_{1,2}}$ as well as the aspect ratio of the torus. They can be computed for arbitrary n_1 and n_2 , but we have not been able to find a closed formula except for very simple cases. For the CF construction we need to know the coefficients for $n_2 = n = 0$, but arbitrary n_1 . In the following, we restrict ourselves to these cases.

In order to simplify notation later on we define Q as the greatest common divisor (\gcd) of N_{ϕ_1} and N_{ϕ_2} :

$$\begin{aligned} Q &= \gcd(N_{\phi_1}, N_{\phi_2}) \\ N_{\phi_1} &= t_1 \cdot Q \\ N_{\phi_2} &= t_2 \cdot Q \\ N_{\phi} &= (t_1 + t_2) \cdot Q \equiv t \cdot Q. \end{aligned} \quad (11)$$

It follows that $Q = \gcd(N_{\phi_1}, N_{\phi}) = \gcd(N_{\phi_2}, N_{\phi})$. The different magnetic lengths are related to t_1 and t_2 by:

$$\begin{aligned} \frac{\ell}{\ell_1} &= \sqrt{\frac{t_1}{t}} \\ \frac{\ell}{\ell_2} &= \sqrt{\frac{t_2}{t}}. \end{aligned} \quad (12)$$

For $n_1 = 0, 1$ the coefficients in (10) become rather simple:

$$C_{j_1, j_2; j}^{0, 0; 0} = \sqrt{\frac{\sqrt{2\Im(\tau)}}{\mathcal{A}(-i\tau)\sqrt{Qt^3t_1t_2}}} \theta_3 \left(\frac{\pi(t_2j_1 - t_1j_2 + \beta t_1t_2Q)}{t_1t_2N_{\phi}} \middle| \exp \left[\frac{\pi}{i\tau t_1t_2N_{\phi}} \right] \right) \quad (13)$$

$$C_{j_1, j_2; j}^{1, 0; 0} = -\sqrt{\frac{\pi\sqrt{2\Im(\tau)^3}}{(-i\tau)^3\mathcal{A}\sqrt{Q^3t^7t_1^3t_2}}} \theta'_3 \left(\frac{\pi(t_2j_1 - t_1j_2 + \beta t_1t_2Q)}{t_1t_2N_{\phi}} \middle| \exp \left[\frac{\pi}{i\tau t_1t_2N_{\phi}} \right] \right), \quad (14)$$

where $j = (j_1 + j_2 + \beta Qt_1) \bmod N_{\phi}$, for $\beta = 0, 1, \dots, t-1$. $C_{j_1, j_2; j}^{0, 0; 0} = C_{j_1, j_2; j}^{1, 0; 0} = 0$ for $j \neq (j_1 + j_2 + \beta Qt_1) \bmod N_{\phi}$. The third θ -function is defined by:

$$\begin{aligned} \theta_3(z|q) &= \theta \begin{bmatrix} 0 \\ 0 \end{bmatrix} (z|q) \\ \theta \begin{bmatrix} a \\ b \end{bmatrix} &= \sum_{k=-\infty}^{\infty} q^{(k+a)^2} e^{2i(k+a)(z+b)} \end{aligned} \quad (15)$$

and $\theta'_3(z|q) = \partial_z \theta_3(z|q)$. For higher n_1 , the coefficients can in principle still be represented with help of higher derivatives of the θ_3 -function, but they become increasingly cumbersome to evaluate. They can be written as:

$$\begin{aligned} C_{j_1, j_2; j}^{n_1 0; 0} &= \frac{\mathcal{N}_{n_1}^{\ell_1} \mathcal{N}_0^{\ell_2}}{\mathcal{N}_0^{\ell}} \sum_{\beta=0}^{t-1} \delta_{j, (j_1 + j_2 + \beta Qt_1) \bmod N_{\phi}} \sum_{i=0}^{\lfloor n_1/2 \rfloor} \binom{n_1}{2i} \frac{(2i)!}{i!} \left(-\frac{t_2}{t} \right)^i \left(-4\pi t_1 t_2 \sqrt{\frac{\Im(\tau)Q}{2\pi t_1}} \right)^{n_1-2i} \\ &\times \sum_{s=-\infty}^{\infty} \left(s - \frac{t_2j_1 - t_1j_2 + \beta t_1t_2Q}{t_1t_2N_{\phi}} \right)^{n_1-2i} \exp \left[i\pi \tau t_1 t_2 N_{\phi} \left(s - \frac{t_2j_1 - t_1j_2 + \beta t_1t_2Q}{t_1t_2N_{\phi}} \right)^2 \right]. \end{aligned} \quad (16)$$

The derivation of Eq. (16) involves straightforward, but tedious algebra, which is done in Appendix A. Eq.s (13)

and (14) can be obtained from (16) by a Poisson resummation. Note that for $\Im(\tau)$ not too small, the summa-

tion over s converges rapidly. For numerical purposes, one needs to care only about the first few terms around zero. The problem of convergence for small $\Im(\tau)$ can in principle be avoided by doing a Poisson resummation on the sum over s —similar to what was done in obtaining Eq.s (13) and (14).

D. Composite fermion wave functions on the torus

The formulas derived in the previous section allow for evaluation of the Jain state at filling $\nu = \frac{n}{np+1}$ given by

$$\Psi_\nu(\{z_j\}) = \mathcal{P}_{LLL} [\Phi_n(\{z_j\}) \cdot \Phi_1(\{z_j\})^p], \quad (17)$$

where Φ_j is the many-body wave function of the lowest j Landau levels completely filled. For p even(odd), this

describes a fermionic (bosonic) state. As a sanity check, one may note that $n = 1$ reproduces the Laughlin states at filling $\frac{1}{p+1}$. Expression (17) can also be used to evaluate wave functions corresponding to quasi-hole and/or quasi-electron excitations—in the same way as on the sphere or the disk. For sake of simplicity, we focus on ground state wave functions in the following discussion.

In principle, it is straightforward to evaluate (17), by multiplying out the slater determinants and using the coefficients (16) (repeatedly if $p > 1$) to reduce the expression to a lowest Landau level wave function at the combined flux. For the simplest state, describing the bosonic Jain state at filling $\nu = 2/3$, the explicit expression becomes:

$$\Psi_{2/3}(\{x_i, y_i\}) = \sum_{\sigma \in S_N} (-1)^\sigma \left(\prod_{\alpha=0}^{N-1} \sum_{\beta_\alpha=0}^2 \right) \prod_{\alpha=0}^{N/2-1} \left(C_{\alpha, \sigma(\alpha); j_\alpha}^{10;0} C_{\alpha, \sigma(\alpha+N/2); j_{\alpha+N/2}}^{00;0} \right) \sqrt{N! \prod_{j=0}^{N_\phi-1} n_j! m_\mu(\{z_j\})}, \quad (18)$$

where $j_\alpha = (\alpha \bmod N_{\phi_1} + \sigma(\alpha) + \beta_\alpha Q t_1) \bmod N_\phi$. The $m_\mu(\{z_j\})$'s are the many-body basis states on the torus:

$$m_\mu(\{z_j\}) = \langle z_1, \dots, z_N | \mu \rangle, \quad (19)$$

with $\mu = \{n_0, \dots, n_{N_\phi-1}\}$ and $n_j = \sum_{\alpha=0}^{N_\phi-1} \delta_{j, j_\alpha}$ being the occupation number of the single-particle orbital with \hat{t}_1 -eigenvalue $\exp[-2\pi i j/N_\phi]$.

The qualitative difference between Eq. (18) to the corresponding disk and sphere expressions lies in the additional sums over β_1, \dots, β_N . In the disk and sphere geometry, the momentum of the product of two single-particle states on the torus is simply the sum of the two momenta. The projection, thus, involves evaluating $N!$ terms in order to obtain the coefficients in the occupation number basis. On the torus, the momentum is only defined modulo the flux N_ϕ . This implies that the winding sums in the single-particle states at flux N_{ϕ_1} and N_{ϕ_2} yield different momenta at the final flux. For instance, in order to compute the CF state at filling fraction $\nu = 2/3$, one needs to evaluate $N!3^N$ terms, which limits the system sizes one can reach. Note that this limitation becomes worse, if we increase p in Eq. (17).

In addition, (17) is in general not an eigenstate of the many-body translation operator $\hat{T}_1 = \prod_{j=0}^{N-1} \hat{t}_1^{(j)}$, where $\hat{t}_1^{(j)}$ translates the j 'th particle by \vec{L}_1/N_ϕ . An eigenstate can be obtained by either restricting to the correct momentum sector in the Fock basis or by applying the appropriate projection operator.

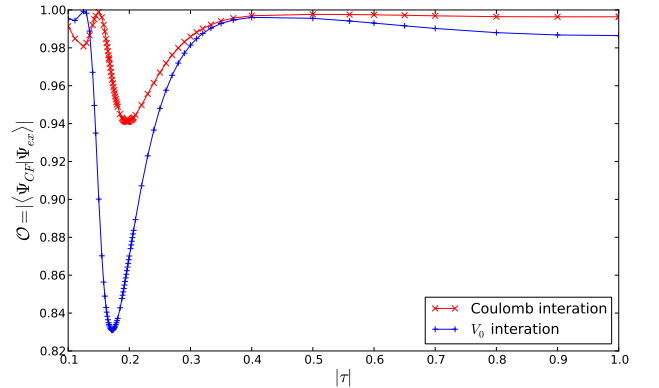


Figure 1: color online: Overlap of CF state at filling $\nu = 2/3$ for $N = 10$ bosons with the exact diagonalization state using Coulomb interaction (red \times) and a contact interaction using the Haldane pseudopotential V_0 (blue $+$). The lines are a guide to the eye.

III. NUMERICAL ANALYSIS

In this section, we present numerical checks on the wave functions obtained by Eq. (17). We computed the overlap between the exact diagonalization ground state and the bosonic CF state at filling $\nu = 2/3$ for system sizes up to 10 particles and in the fermionic case at filling $\nu = 2/5$ for system sizes up to $N = 6$ particles. The exact

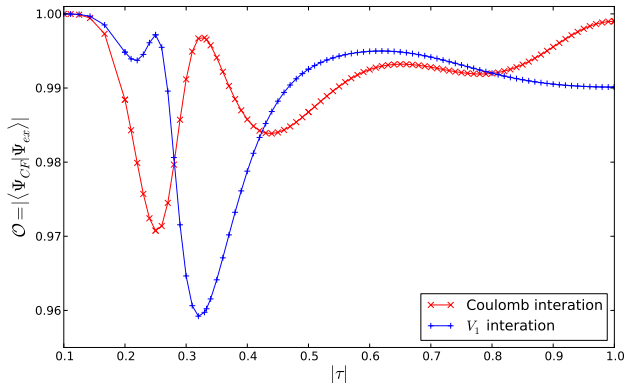


Figure 2: color online: Overlap of CF state at filling $\nu = 2/5$ for $N = 6$ electrons with the exact diagonalization ground state using Coulomb interaction (red \times) and a short-range interaction using the Haldane pseudopotential V_1 (blue $+$). The lines are a guide to the eye.

diagonalization was done both for Coulomb interaction and the smallest relevant Haldane pseudopotential [6]— V_0 for bosons and V_1 for fermions. The shape of the torus was kept rectangular ($\theta = \frac{\pi}{2}$ in Eq. (4)), with aspect ratios $|\tau|$ varying from 0.1 to 10. Due to the invariance of the shape of the torus under the modular transformation $\mathcal{S} : \tau \rightarrow -1/\tau$, we can restrict the analysis to aspect ratios $0.1 \leq |\tau| \leq 1$ without loss of generality, as a torus with $|\tau| > 1$ can be obtained by an \mathcal{S} -transformation. The absolute value of the overlap $\mathcal{O} = |\langle \Psi_{CF} | \Psi_{ex} \rangle|$ between the CF state and the exact diagonalization ground state is shown in figures 1 and 2 for varying aspect ratios.

When comparing overlaps of the torus and sphere geometry, we choose the most isotropic point, namely the square torus with $|\tau| = 1$. In the bosonic case, we find an overlap of $\mathcal{O} = 0.996$ (Coulomb interaction) and $\mathcal{O} = 0.973$ (V_0 -interaction) for a square torus, which are slightly higher than the overlaps found in Ref. [30] for the spherical geometry. In the fermionic case, we find overlaps $\mathcal{O} = 0.999$ (Coulomb interaction) and $\mathcal{O} = 0.990$ (V_1 -interaction), which are slightly lower, but still comparable to the overlaps found in Ref. [31].

The overlaps depend strongly on the shape of the torus, even though they remain quite high throughout the whole range of aspect ratios. On general grounds, we expect the overlap to approach unity in the limit of $|\tau| \rightarrow 0$ and $|\tau| \rightarrow \infty$. In Ref. [32] it was shown that the ground state of Hamiltonians with quite generic repulsive interactions becomes a product state for aspect ratios $|\tau| \rightarrow \infty$ —the so-called thin torus limit. We checked numerically that the CF state has this property as well. The other limit $|\tau| \rightarrow 0$ can—for a rectangular torus—be mapped to the thin torus limit, when using the Landau gauge $\tilde{A} = Bx\hat{y}$ and eigenfunctions of the \hat{t}_2 -operator.

For all system sizes, we observe a dip (in case of fermions several dips) in the overlap curve. The posi-

tion of these dips depends on the system size—in the bosonic case, it seems to be shifted to lower values of $|\tau|$ for increasing system size. In the fermionic case, there is too little numerical data to make a statement. The origin of the dips is not clear at the moment, but one can note that the overlap of the fermionic Laughlin state at $\nu = 1/3$ with the Coulomb ground state has a qualitatively similar behaviour as a function of $|\tau|$ to the one shown in figure 2.

IV. PROJECTION SCHEMES IN REAL SPACE

In principle, the method described in this manuscript allows one to compute any CF states on the torus. However, evaluating Eq. (17) becomes numerically hard for large p when using Eq. (10). On the torus, one needs to evaluate $(N!)^p t^N$ terms to obtain the wave function in Fock space. Even on the disk and the sphere, where one does not have the additional complication of the β_1, \dots, β_N sums, the number of terms, which one needs to evaluate, is still $(N!)^p$. This restricts the system size to very small systems for large p .

A way around this, at least on the disk and the sphere, is to evaluate Eq. (17) in real space and use Monte Carlo techniques to study the resulting model wave functions. How to write the projection operator \mathcal{P}_{LLL} in real space was shown by Girvin and Jach in Ref. [29]. It amounts to moving all anti-holomorphic components to the left and replacing them by derivative operators $\bar{z} \rightarrow 2\frac{\partial}{\partial \bar{z}}$ with the assumption that the derivatives do not act on the Gaussian factors.

This simple implementation of the projection has no straightforward analog on the torus. Note that derivatives are not valid operators on the torus, because they destroy the periodic boundary conditions (7). Following Ref. [18] one may argue that the torus analog to the derivative operator should be related to the small translation operators \hat{t}_1 and \hat{t}_2 (6), because the small translation operators keep the boundary conditions intact and become effectively holomorphic derivatives in the limit $L_1, L_2, N_\phi \rightarrow \infty$. In fact, the analog of the derivative operators may be given by a sum of translation operators that have good modular properties [19]. It is an open question whether or not this idea could be used also to simplify the evaluation of the CF torus wave functions. As a modular invariant sum necessarily involves N_ϕ^2 terms [33], this projection scheme would be numerically cheaper than the one used here only if the sum over different translations converge rapidly.

A numerically very efficient way to evaluate Eq. (17) approximately is the Jain-Kamilla projection [34, 35]. The Jain-Kamilla projection is a close approximation to the exact projection, but can—in contrast to the latter—be evaluated for very large system sizes. It amounts to

dividing the Jastrow factor in Eq. (1) as

$$\prod_{i < j} (z_i - z_j)^{2p} \sim \prod_{i \neq j} (z_i - z_j)^p \quad (20)$$

and multiplying each column α of the slater determinant $\Phi_n(\{z_j\})$ by $\prod_{j \neq \alpha} (z_\alpha - z_j)^p$. Then, each component of the slater determinant is projected separately to the lowest Landau level by

$$\partial_\alpha \prod_{j \neq \alpha} (z_\alpha - z_j)^p = \sum_{j \neq \alpha} \frac{p}{z_\alpha - z_j} \prod_{j \neq \alpha} (z_\alpha - z_j)^p. \quad (21)$$

When trying to generalize this scheme to the torus, one may note that the effect of the derivative operators in (21) is to remove zeroes between particles. On the torus, we cannot remove zeroes but we may shift them. This is in fact exactly, what the translation operators do, that were mentioned in the previous section,. However, one needs to shift the zeroes without destroying the boundary conditions. The most straightforward implementation of (21) would, thus, require a doubly periodic function with only a single pole, which— as we know from complex analysis— does not exist. Unfortunately, the boundary conditions impose rather strict rules on how one may change the wave function, which is why we have not been able to find an analog of the Jain-Kamilla projection on the torus.

V. SUMMARY

In this manuscript, we generalized the CF theory to the torus geometry. We showed the validity of our method by calculating the overlap between the CF states and the exact diagonalization ground state of Coulomb and the smallest relevant Haldane-pseudopotential interactions for filling fractions $\nu = 2/3$ and $\nu = 2/5$ and system sizes up to $N = 10(6)$ particles for the bosonic (fermionic) states. The overlaps on the square torus are

comparable to the ones obtained in the disk and sphere geometry. It turns out that numerical evaluation of the wave function is harder on the torus than on the disk and sphere, because the winding sums mix different momentum sectors. We have also speculated on possible generalizations of the real space projection schemes to the torus geometry, though, unfortunately, we have not been able to find an explicit realization. Such schemes may allow one to reach larger system sizes than are possible with the method presented here.

Let us emphasize again that our method works for the whole low-energy sector of the CF states, even though we only treated the ground states explicitly in this article. The techniques introduced here may be useful for systems that cannot be studied directly on the sphere, because they have different shifts, as eg. the one studied in Ref. [36]. They can also be used to study generalizations of the abelian Haldane-Halperin hierarchy, such as the BS states [26], the NAC state [27], or the bipartite CF states [28]. Also it will clearly be interesting to see whether the exact agreement between the hierarchy and the CF wave functions that have been demonstrated on the plane and on the sphere, also holds true on the torus.

Acknowledgements The author wants to thank Steve Simon, Mike Stone, and Nicolas Regnault for interesting discussions and Hans Hansson for interesting discussions and a critical reading of the manuscript. The exact diagonalization ground states were computed using DiagHam. The author wants to thank all contributors to the code, especially Nicolas Regnault.

Appendix A: Derivation of product formula

In this appendix, we derive formula (16) for an expansion of the product of two single-particle states at fluxes N_{ϕ_1} and N_{ϕ_2} in terms of the single-particle states at the combined flux N_ϕ with $N_{\phi_1} + N_{\phi_2} = N_\phi$. The product of two single-particle states is given by:

$$\begin{aligned} \phi_{n_1, j_1}^{\ell_1}(x, y) \cdot \phi_{0, j_2}^{\ell_2}(x, y) &= \mathcal{N}_{n_1} \mathcal{N}_0 e^{-y^2/(2\ell^2)} \sum_{k_1=-\infty}^{\infty} \sum_{k_2=-\infty}^{\infty} e^{-2\pi i (j_1 + k_1 N_{\phi_1} + j_2 + k_2 N_{\phi_2}) z} \\ &\times \exp \left[i\pi \tau \left(\frac{(j_1 + k_1 N_{\phi_1})^2}{N_{\phi_1}} + \frac{(j_2 + k_2 N_{\phi_2})^2}{N_{\phi_2}} \right) \right] \cdot H_{n_1} \left(\frac{2\pi\ell_1}{L_1} (j_1 + k_1 N_{\phi_1}) - \frac{y}{\ell_1} \right). \end{aligned} \quad (A1)$$

In the following, subscript 1 and 2 denote quantities of the two single-particle states respectively, while those without subscript denote those of the product. Note that $N_\phi = N_{\phi_1} + N_{\phi_2}$ and $\ell^{-2} = \ell_1^{-2} + \ell_2^{-2}$. Let us assume $n_2 = 0$ but n_1 may be arbitrary for the time being. We could also consider arbitrary n_2 , but it will only compli-

cate things unnecessarily.

Define Q as the greatest common divisor (gcd) of N_{ϕ_1} and N_{ϕ_2} :

$$\begin{aligned} Q &= \gcd(N_{\phi_1}, N_{\phi_2}) \\ N_{\phi_1} &= t_1 \cdot Q \\ N_{\phi_2} &= t_2 \cdot Q \\ N_{\phi} &= (t_1 + t_2) \cdot Q \equiv t \cdot Q. \end{aligned} \quad (\text{A2})$$

It follows that $Q = \gcd(N_{\phi_1}, N_{\phi}) = \gcd(N_{\phi_2}, N_{\phi})$. We use that the different magnetic lengths are related as :

$$\begin{aligned} \frac{\ell}{\ell_1} &= \sqrt{\frac{t_1}{t}} \\ \frac{\ell}{\ell_2} &= \sqrt{\frac{t_2}{t}}. \end{aligned} \quad (\text{A3})$$

We define the torus as in Section II. It is easy to check that the product of the two single-particle states obeys the correct boundary conditions for flux N_{ϕ} .

Let us first discuss how to rewrite the double sum over windings coming from both single-particle states, denoted by k_1 and k_2 . We can choose integers $k, s \in \mathbb{N}$, and $\beta \in \{0, \dots, t-1\}$ such that

$$\begin{aligned} k_1 &= \beta + k - t_2 s \\ k_2 &= k + t_1 s, \end{aligned} \quad (\text{A4})$$

which implies

$$\begin{aligned} t \cdot k &= t_1 k_1 + t_2 k_2 + \beta \\ t \cdot s &= \beta + k_2 - k_1. \end{aligned} \quad (\text{A5})$$

It is beneficial to introduce some more notation, that will simplify expressions later on. We find that we can rewrite the phase factors of the single-particle states as

$$\begin{aligned} j_1 + k_1 N_{\phi_1} &= \frac{\ell^2}{\ell_1^2} A_k - t_1 t_2 Q \cdot Y_s \\ j_2 + k_2 N_{\phi_2} &= \frac{\ell^2}{\ell_2^2} A_k + t_1 t_2 Q \cdot Y_s, \end{aligned} \quad (\text{A6})$$

where A_k depends only on k and β , but not on s , while Y_s depends only on s and β , but not on k :

$$\begin{aligned} A_k &= j_1 + j_2 + k N_{\phi} + \beta t_1 Q. \\ Y_s &= s - \frac{t_2 j_1 - t_1 j_2 + \beta t_1 t_2 Q}{t_1 t_2 N_{\phi}}. \end{aligned} \quad (\text{A7})$$

Using these definitions we see that the z -dependent factor on the right-hand-side of Eq. (A1) does not depend on the summation index s and becomes rather simple:

$$e^{-2\pi i(j_1 + k_1 N_{\phi_1} + j_2 + k_2 N_{\phi_2})z} = e^{-2\pi i A_k z}. \quad (\text{A8})$$

Let us now consider the factor that is exponential in the winding number. Using (A7) it can be rewritten as

$$\begin{aligned} &\exp \left[i\pi\tau \left(\frac{(j_1 + k_1 N_{\phi_1})^2}{N_{\phi_1}} + \frac{(j_2 + k_2 N_{\phi_2})^2}{N_{\phi_2}} \right) \right] \\ &= \exp \left[i\pi\tau \left(\frac{A_k^2}{N_{\phi}} + t_1 t_2 N_{\phi} Y_s^2 \right) \right] \end{aligned} \quad (\text{A9})$$

ie. it factorizes into two parts, each of which only depends on one of the summation indices.

Most of the complication lies in the Hermite polynomials, at least if $n_1 \neq 0, 1$. The Hermite polynomial in Eq. (A1) can be written as

$$\begin{aligned} H_{n_1} \left(\frac{2\pi\ell_1}{L_x} (j_1 + k_1 N_{\phi_1}) - \frac{y}{\ell_1} \right) &= \\ H_{n_1} \left(\frac{\ell}{\ell_1} \left[\frac{2\pi\ell}{L_x} \cdot A_k - \frac{y}{\ell} \right] - \left(\frac{2\pi\ell_1}{L_x} t_1 t_2 Q \right) Y_s \right). \end{aligned} \quad (\text{A10})$$

With the following identities

$$\begin{aligned} H_n(x+y) &= \sum_{k=0}^n \binom{n}{k} H_k(x) \cdot (2y)^{n-k} \\ H_k(\gamma x) &= \sum_{i=0}^{\lfloor k/2 \rfloor} \gamma^{k-2i} (\gamma^2 - 1)^i \binom{k}{2i} \frac{(2i)!}{i!} \cdot H_{k-2i}(x) \end{aligned} \quad (\text{A11})$$

we find that

$$\begin{aligned} H_{n_1} \left(\frac{\ell}{\ell_1} \frac{2\pi\ell}{L_1} A_k - \alpha_1 Y_s \right) &= \\ &= \sum_{l=0}^{n_1} \binom{n_1}{l} (-2\alpha_1 Y_s)^{n_1-l} \cdot H_l \left(\frac{\ell}{\ell_1} \frac{2\pi\ell}{L_1} A_k \right) \\ &= \sum_{l=0}^{n_1} \sum_{i=0}^{\lfloor l/2 \rfloor} \frac{(2i)!}{i!} \left(\frac{\ell}{\ell_1} \right)^{l-2i} \left(-\frac{\ell^2}{\ell_2^2} \right)^i \binom{l}{2i} \binom{n_1}{l} \\ &\quad \times (-2\alpha_1 Y_s)^{n_1-l} \cdot H_{l-2i} \left(\frac{2\pi\ell}{L_1} A_k \right) \end{aligned} \quad (\text{A12})$$

where $\alpha_1 = 2\pi\ell_1 t_1 t_2 Q / L_1$ and $\lfloor k/2 \rfloor = k/2$ if k is even, resp. $(k-1)/2$ if k is odd. The first line in Eq. (A11) can easily be derived using the generating function of the Hermite polynomials. The second is more tedious to derive and follows from successive partial integration of the integral $\int dx \exp[-x^2] H_n(\gamma x) H_m(x)$.

We can now identify the coefficient $C_{j_1, j_2; j}^{n_1; n}$ to be

$$C_{j_1,j_2;j}^{n_1,0;n} = \frac{\mathcal{N}_{n_1}^{\ell_1} \mathcal{N}_0^{\ell_2}}{n! \mathcal{N}_n^{\ell}} \sqrt{\frac{t_1}{t}}^n \sum_{i=0}^{\lfloor (n_1-n)/2 \rfloor} \frac{n_1!}{(n_1-n-2i)! i!} \left(-\frac{t_2}{t}\right)^i \left(-4\pi t_1 t_2 \sqrt{\frac{\Im(\tau)Q}{2\pi t}}\right)^{n_1-n-2i} \times \sum_{s=-\infty}^{\infty} \left(s - \frac{t_2 j_1 - t_1 j_2 + \beta t_1 t_2 Q}{t_1 t_2 N_\phi}\right)^{n_1-n-2i} \exp\left[i\pi\tau t_1 t_2 N_\phi \left(s - \frac{t_2 j_1 - t_1 j_2 + \beta t_1 t_2 Q}{t_1 t_2 N_\phi}\right)^2\right] \quad (\text{A13})$$

where $j = (j_1 + j_2 + \beta t_1 Q) \bmod N_\phi$. The coefficients vanish for other values of j . Eq. (16) is obtained by

setting $n = 0$. In order to find Eq.s (13) and (14) one must do a Poisson resummation on the sum over s .

[1] D.C. Tsui, H. L. Stoermer, and A. C. Gossard, Phys. Rev. Lett. **51**, 605 (1983).

[2] J.M. Leinaas and J. Myrheim, Il Nuovo Cimento B **37** 1-23 (1977).

[3] X.-G. Wen, Advances in Physics, **44**, 405 (1995).

[4] R.B. Laughlin, Phys. Rev. Lett. **50**, 1395 (1983).

[5] H. Li and F.D.M. Haldane, Phys. Rev. Lett. **101**, 010504 (2008).

[6] F.D.M. Haldane, Phys. Rev. Lett. **51**, 605 (1983).

[7] B.I. Halperin, Phys. Rev. Lett. **52**, 1583, 2390 (1984).

[8] J. K. Jain, Phys. Rev. Lett. **63**, 199 (1989).

[9] E. J. Bergholtz, T. H. Hansson, M. Hermanns, A. Karlhede, and S. Viefers, Phys. Rev. B **77**, 165325 (2008).

[10] J. Suorsa, S. Viefers, and T. H. Hansson, Phys. Rev. B **83**, 235130 (2011).

[11] T.H. Hansson, C.-C. Chang, J.K. Jain, S. Viefers, Phys. Rev. Lett. **98**, 076801 (2007).

[12] T.H. Hansson, M. Hermanns, and S. Viefers, Phys. Rev. B **80**, 165330 (2009).

[13] T. Kvorning, arXiv:1302.3808 (2013).

[14] J. K. Jain, Composite Fermions (Cambridge University Press, 2007).

[15] F.D.M. Haldane and E.H. Rezayi, Phys. Rev. B **31**, 2529 (1985).

[16] N. Read and E. Rezayi, Phys. Rev. B **54**, 16864-16887 (1996).

[17] S.B. Chung, M. Stone, J. Phys. A **40**, 4923 (2007).

[18] M. Hermanns, J. Suorsa, E.J. Bergholtz, T.H. Hansson, and A. Karlhede, Phys. Rev. B **77**, 125321 (2008).

[19] T.H. Hansson, private communication, and talk at APS march meeting (2013). <http://meetings.aps.org/link/BAPS.2013.MAR.R23.4>

[20] G. Moore and N. Read, Nucl. Phys. B **360**, 362 (1991).

[21] B.I. Halperin, P.A. Lee, and N. Read, Phys. Rev. B **47**, 7312 (1993).

[22] E.H. Rezayi and F.D. Haldane, Phys. Rev. Lett. **84**, 4685 (2000).

[23] A.M. Laeuchli, E.J. Bergholtz, J. Suorsa, and M. Haque, Phys. Rev. Lett. **104**, 156404 (2010).

[24] J. E. Avron, R. Seiler, and P. G. Zograf, Phys. Rev. Lett. **75**, 697 (1995).

[25] N. Read, Phys. Rev. B **79**, 045308 (2009).

[26] P. Bonderson, J. K. Slingerland, Phys. Rev. B **78**, 125323 (2008).

[27] M. Hermanns, Phys. Rev. Lett. **104**, 056803 (2010).

[28] G.J. Sreejith, C. Toke, A. Wojs, and J. K. Jain, Phys. Rev. Lett. **107**, 086806 (2011).

[29] S. Girvin and T. Jach, Phys. Rev. B **29**, 5617 (1984).

[30] C.-C. Chang, N. Regnault, T. Joliceur, and J.K. Jain, Phys. Rev. A **72**, 013611 (2005).

[31] G. Dev and J.K. Jain, Phys. Rev. Lett. **69**, 2843 (1992).

[32] E.J. Bergholtz and A. Karlhede, Phys. Rev. B **77**, 155308 (2008).

[33] F.D.M. Haldane, Phys. Rev. Lett **55**, 2095 (1985).

[34] J. K. Jain and R. K. Kamilla, Int. J. Mod. Phys. B **11**, 2621 (1997).

[35] J. K. Jain and R. K. Kamilla, Phys. Rev. B **55**, 4895 (1997).

[36] M. V. Milovanovic and Z. Papić, Phys. Rev. B **82**, 035316 (2010).

[37] One can of course remedy the first problem by adding the appropriate center-of-mass pieces 'by hand'. However, in contrast to the Laughlin case we do not expect the center-of-mass piece to be uniquely defined for given many-body momentum as there are no model Hamiltonians with the Jain states as unique exact ground states.